

The Tumorigenic Diversity of the Three PLAG Family Members Is Associated with Different DNA Binding Capacities¹

Karen Hensen, Isabelle C. C. Van Valckenborgh, Koen Kas, Wim J. M. Van de Ven, and Marianne L. Voz

Laboratory for Molecular Oncology, Center for Human Genetics (CME), University of Leuven (KUL) and Flanders Interuniversity Institute for Biotechnology (VIB), Herestraat 49 B-3000 Leuven, Belgium

ABSTRACT

Pleomorphic adenoma gene (PLAG) 1, the main translocation target in pleomorphic adenomas of the salivary glands, is a member of a new subfamily of zinc finger proteins comprising the tumor suppressor candidate *PLAG-like1* (also called *ZAC1* or *lost on transformation 1*) and *PLAGL2*. In this report, we show that NIH3T3 cells overexpressing *PLAG1* or *PLAGL2* display the typical markers of neoplastic transformation: (a) the cells lose cell-cell contact inhibition; (b) show anchorage-independent growth; and (c) are able to induce tumors in nude mice. In contrast, *PLAGL1* has been shown to prevent the proliferation of tumor cells by inducing cell cycle arrest and apoptosis. This difference in function is also reflected in their DNA binding, as we show here that the three PLAG proteins, although highly homologous in their DNA-binding domain, bind different DNA sequences in a distinct fashion. Interestingly, the *PLAG1*- and *PLAGL2*-induced transformation is accompanied by a drastic up-regulation of *insulin-like growth factor-II*, which we prove is a target of *PLAG1* and *PLAGL2*. This strongly suggests that the oncogenic capacity of *PLAG1* and *PLAGL2* is mediated at least partly by activating the *insulin-like growth factor-II* mitogenic pathway.

Abbreviations : PLAG, pleomorphic adenoma gene; IGF, insulin-like growth factor; ORF, open reading frame; β -gal, β -galactosidase; EMSA, electrophoretic mobility shift analysis; IGF-I-R, type 1 insulin-like growth factor.

INTRODUCTION

Pleomorphic adenoma of the salivary gland is a benign epithelial tumor, which usually arises as a result of activation of the *PLAG1* gene on chromosome 8q12 (1). In most cases, this activation results from recurrent chromosomal translocations that lead to promoter substitution between *PLAG1*, a gene mainly expressed in fetal tissue, and more broadly expressed genes. The three translocation partners characterized thus far are the β -catenin gene (1), the *leukemia inhibitory factor receptor* gene (2), and the elongation factor *SII* gene (3). Breakpoints invariably occur in the 5' noncoding part of the *PLAG1* gene, leading to an exchange of regulatory control elements while preserving the *PLAG1* coding sequence. The replacement of the *PLAG1* promoter, which is inactive in adult salivary glands, by a strong promoter derived from the translocation partner, leads to ectopic expression of *PLAG1* in the tumor cells. This abnormal *PLAG1* expression presumably results in a deregulation of *PLAG1* target genes, causing salivary gland tumorigenesis.

We demonstrated recently that *PLAG1* is a genuine transcription factor that binds a bipartite element containing a Core sequence, GRGGC, and a G-cluster, RGGK, separated by seven random nucleotides. Potential *PLAG1*-binding sites were found in promoter 3 of the human *IGF-II* gene. Remarkably, *IGF-II* transcripts deriving from the P3 promoter are highly expressed in salivary gland adenomas overexpressing *PLAG1*, whereas they are not detectable in adenomas without abnormal *PLAG1* expression or in normal salivary gland tissue. This suggests that *IGF-II* could be a *PLAG1* target gene (4).

Two novel cDNAs encoding C₂H₂ zinc finger proteins, *PLAGL1* and *PLAGL2*, which show high homology to

¹ The costs of publication of this article were defrayed in part by the payment of page charges. This article must therefore be hereby marked *advertisement* in accordance with 18 U.S.C. Section 1734 solely to indicate this fact.

Supported by the "Geconcerteerde Onderzoekacties 1997-2001" and the "Fonds voor Wetenschappelijk Onderzoek Vlaanderen (FWO)." M. L. V. is a Chercheur Qualifié from the Fonds National de la Recherche Scientifique, I. C. C. V. is an aspirant fellow of the FWO, and K. H. is a doctoral fellow of the VIB.

PLAG1, have been identified, constituting by this way a novel subfamily of zinc finger proteins (5). *PLAGL1* has also been isolated independently and referred to as *LOT1* and *ZAC1* (6, 7). The homology between these three PLAG proteins resides mainly in their NH₂-terminal zinc finger domain (73% and 79% identity for *PLAGL1* and *PLAGL2*, respectively), whereas the COOH-terminal region is much more divergent. Although *PLAGL1* show high homology to *PLAG1* in the DNA-binding domain, the DNA-binding specificities of these two proteins seem to differ slightly. Indeed the consensus binding site for *PLAGL1* has been identified as the sequence GGGGGGCC (8). This sequence contains the extended *PLAG1* core GGRGGCC but does not include the G-Cluster 7 nucleotides downstream. A second difference between these two related factors is that *PLAG1*, when consistently overexpressed in pleomorphic adenomas, is thought to act as a proto-oncogene, whereas *PLAGL1* seems to act as a tumor suppressor gene. Indeed, expression of *PLAGL1* prevented proliferation of tumor cells as measured by colony formation, growth rate, and cloning in soft agar, and precluded tumor formation in nude mice (7, 8). Moreover it encodes a protein that regulates apoptosis and cell cycle arrest (7), maps to a chromosomal region frequently lost in cancer (6), and a decrease or loss of expression has been observed in breast tumors (9).

To determine whether *PLAG1* is a genuine proto-oncogene, we evaluated the *in vitro* transforming capacity of *PLAG1* by analyzing the growth profile of NIH3T3 cells overexpressing *PLAG1*, their ability to form foci, to grow in soft agar, and to form tumors in nude mice. These analyses were extended to *PLAGL1*, the third member of the *PLAG* family. Both *PLAG1* and *PLAGL2* are able to transform NIH3T3 cells and, therefore, can be considered proto-oncogenes. Furthermore, by investigating the DNA binding specificities of the PLAG proteins and comparing their mode of DNA recognition, we demonstrate that *PLAG1* and *PLAGL2* have indistinguishable binding capacities, which are different from that of *PLAGL1*. Their similar binding capacities are reflected in their ability to induce common target genes; we prove here that *IGF-II* is a common target of *PLAG1* and *PLAGL2*. Moreover, the transformation of NIH3T3 cells by these factors is accompanied by a drastic up-regulation of *IgfIII* expression, suggesting that *PLAG1* and *PLAGL2* stimulate cell proliferation by activating the *IGF-II* mitogenic pathway.

MATERIALS AND METHODS

Plasmid Construction. pCDNA3-FLAG-*PLAG1* (=pKH26) was constructed by ligating in frame the *MscI/XhoI* fragment isolated from the pCDNA3-*PLAG1* expression construct (4) into pCDNA3.1FLAG (a kind gift of Stefan Pype of the laboratory of Cell Growth, Differentiation and Development, KUL, VIB). This enables expression of a chimeric protein containing the FLAG epitope fused to amino acids 2-500 of *PLAG1*. The complete *PLAGL2* ORF except the first ATG was amplified using *pyrococcus furiosus* (pfu) DNA polymerase (Stratagene) with the sense primer P3N2 (5'-CCCGAATTCTGACCACATTTTTTCACCAGCG3') and the antisense primer P3C496 (5'-TTTCCATCAAGCATTCCAGTAGCTCGAG3'). The PCR product was cloned in frame into the pCDNA3.1FLAG vector (=pKH32). pMSCV-FLAG-*PLAG1* and pMSCV-FLAG-*PLAGL2* were constructed by cloning a blunt *NheI/XbaI* fragment of pKH26 or pKH32 into the *HpaI* site of the pMSCVpuro retroviral vector, respectively (kindly provided by Jan Cools, CME and KUL, and described by Ref. 10).

The *PLAG1* expression construct pCDNA3-*PLAG1* has been described elsewhere (4). Expression plasmids pCDNA3-*PLAGL1* and pCDNA3-*PLAGL2* were constructed by inserting into *EcoRI-XhoI* digested pCDNA3 (Invitrogen) the complete ORFs of *PLAGL1* or *PLAGL2* including their own Kozak consensus translation start site. These fragments were generated by PCR using pfu polymerase (Stratagene) with the 5' primer P2N-3 (5'-CCCGAATTTCGCAAAGC-CCATGGCCACGTTTC-3') and the 3' primer P2C463 (5'-GGGCTCGAGT-TATCTGAATGCATGATGGAAATGAG-3') for *PLAGL1* and with the 5' primer P3N-3 (5'-CCCGAATTCAGCCTTGCCATGACCACATTT-3') and the 3' primer P3C496 (5'-GGGCTCGAGCTACTGGAATGCTTGATGGAAA-3') for *PLAGL2*. The three mutant PLAG cDNAs (*PLAG1*-F3mut, *PLAGL1*-F3mut, and *PLAGL2*-F3mut) were produced by altering the first codon for the histidine in the C₂H₂ motif of the corresponding zinc finger to that for alanine. This was performed using the QuickChange Site-directed Mutagenesis kit (Stratagene) according to the instructions of the supplier. The pSAR-MT-FLAG-*PLAG1* and pSAR-MT-FLAG-*PLAGL2* constructs were generated by inserting the *NheI/XbaI*-blunted fragments of pKH26 and pKH32, respectively, into the blunted *BamHI* site of the pSAR-MT vector (11). (WT₂)₃-TK-luc and (mCLUmCO₂)₃-TK-luc have been obtained by inserting three copies of the corresponding double-stranded oligonucleotides WT2 and mCOMCLU2 (4) into pTK81luc (12). All of the constructs were sequenced to confirm the fidelity of the PCR and the site-specific mutagenesis.

Cell Lines. The human fetal kidney epithelial cell line 293 (ATCC CRL 1573) was cultured according to the suppliers' protocols. Inducible *PLAG1*-, *PLAGL2*-, and β -gal-expressing cell lines were obtained by transfecting 293 cell line with 2 μ g of pSAR-MT-FLAG-*PLAG1*, pSAR-MT-FLAG-*PLAGL2* or pSAR-MT- β -gal (11),

respectively, together with 400 ng of the neomycin resistance vector pCDNA3 using FuGENE 6 Transfection Reagent (Boehringer Mannheim) according to the manufacturer's protocol. After 10 days, selection with G418 (Life Technologies, Inc.) at a concentration of 700 $\mu\text{g/ml}$, individual clones were isolated and expanded. Individual colonies were screened for zinc-inducible expression of PLAG1, PLAGL2, or β -gal by Western blot analysis. Cells were induced with 100 μM of ZnCl_2 for 16 h.

The pMSCV retroviral constructs were cotransfected with the pIK 6.1 Ecopac vector (kindly provided by Jan Cools, CME, KULeuven), coding for the gag, pol, and env viral proteins, in 293T cells using Superfect (Qiagen) according to the manufacturer's protocol. After transfection (48 h), 1 ml of the supernatant containing replication-incompetent retroviruses was used to infect NIH3T3 cells (ATCC CRL1658). Cells expressing the gene of interest were obtained after 2 days culturing under puromycin selection.

Western Blot Analysis. Cells were harvested in PBS/EDTA. The cell pellets were lysed in SDS-PAGE sample buffer [60 mM Tris-HCl (pH 6.8), 12% glycerol, and 4% SDS], and sonicated. Samples containing equal protein amounts were heated at 95°C for 5 min, and were electrophoresed in a 10% polyacrylamide gel and blotted onto nitrocellulose membranes. FLAG-tagged proteins were detected with a mouse anti-FLAG monoclonal antibody (SIGMA; 0.8 $\mu\text{g/ml}$) followed by a peroxidase-labeled rabbit α -mouse polyclonal antibody (PROSAN; DAKO; 0.4 $\mu\text{g/ml}$). Blots were revealed using the Renaissance detection kit (NEN Life Science Products) according to the supplier's instructions.

Transfections and Luciferase Assay. The puromycin-resistant cells, obtained after infection with recombinant retroviruses or empty pMSCV vectors, were plated in six-well plates. The next day, they were transiently cotransfected in triplicate with 400 ng of (WT2)₃TKluc or (mCLUmCO₂)₃TKluc reporter plasmids together with the Rouse sarcoma virus β -gal DNA as internal control using 3 μl of FuGENE 6 Transfection Reagent (Boehringer Mannheim) according to the manufacturer's protocol. Cells were harvested 40 h after the transfection and luciferase activity measured using a Monolight 2010 luminometer (Analytical Luminescence Laboratory).

Preparation of RNA and Northern Blot Analysis. Total RNA was extracted using the guanidine thiocyanate method (13). Northern blot analysis was performed according to standard procedures. For filter hybridizations, probes were radiolabeled with α [³²P]dCTP using the megaprime DNA labeling system (Amersham). A 1.5-kb cDNA probe containing the complete *PLAG1* or *PLAGL2* ORF was used for the detection of the respective transcripts. A probe containing exon 6 of the mouse *IgfII*, which is common to the different transcripts generated by the three different promoters, was generated by PCR using sense primer mIgfII-up (5'CAGATACCCCGTGGGCAAGTTCCTC-CAATA3') and antisense primer mIgfII-low (5'TGAAGGGGGGGGGCGC-CGAATTATTTGA3'). The human *IGF-II* exon 9 probe, common to the four different transcripts P1, P2, P3, and P4, was generated by PCR and contained nucleotides 7970-8774 of the published gene sequence (Ref. 14; GenBank/European Molecular Biology Laboratory; accession no. X03562). A human *IGF-II* exon 5 probe specific for the P3 transcript was a kind gift of Dr. P. E. Holthuisen. The lacZ probe was generated by isolation of a 2.3-kb *Clal-EcoRI* fragment from SDKlacZpA (Ref. 15; kindly given by Dr. J. Rossant).

EMSA. The full-length PLAG proteins as well as the mutants were expressed by *in vitro* transcription and translation using the TNT kit (Promega). Quality of translation was monitored by SDS PAGE analysis of [³⁵S]Met-labeled proteins. The EMSAs were performed as described previously (4) and 3 μl of translation reaction products were used per lane.

Focus Formation Assay. Puromycin-resistant cells, obtained after infection with recombinant retroviruses, were plated at a density of 3×10^5 cells in a 60-mm tissue culture dish and grown in DMEM/F12 medium supplemented with 10% or 1% FCS and puromycin. Medium was changed every 2 or 3 days, and foci of densely growing cells appeared after 2-3 weeks. Some of the foci were cloned and grown to mass culture for RNA and protein analysis.

Cell Proliferation Assay. Puromycin-resistant cells, obtained after infection with recombinant retroviruses, were plated at a density of 1×10^5 cells in a 60-mm tissue culture dish and cultured in of 5% or 1% FCS. Cells were counted every day for 10 days using a Coulter counter.

Soft Agar Assay. Puromycin-resistant cells (1×10^5), obtained after infection with recombinant retroviruses, were resuspended in 2 ml 0.3% agar/DMEM/15%FCS and plated on a base of 0.6% agar/DMEM/15% FCS in six-well plates. After 5 days the cells were fed with a fresh agar overlay in DMEM containing 15% FCS.

Colonies were counted 3 weeks after plating.

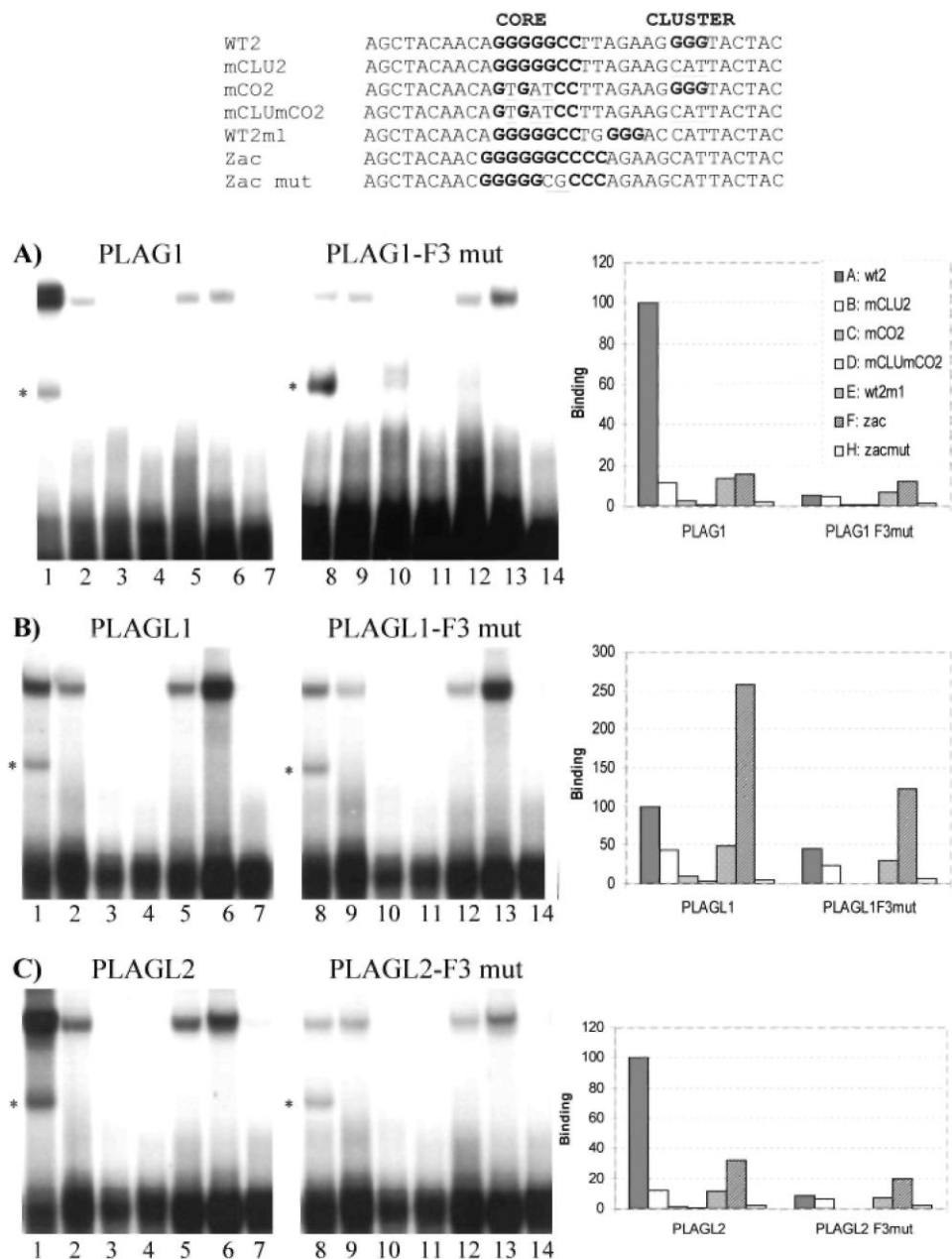
Tumorigenicity in Nude Mice. Tumorigenicity was evaluated by injecting the puromycin-resistant cells, obtained after infection with recombinant retroviruses carrying pMSCV-FLAG-PLAG1, pMSCV-FLAG-PLAGL2, or empty pMSCV vectors (5×10^6 cells in 0.1 ml PBS) s.c. into both flanks of athymic nude mice. The mice were examined for tumor development once a week for 2 months. All of the tumors were clearly macroscopically visible within 3-4 weeks after inoculation. Mice were sacrificed after 5 weeks, and the tumors were excised for RNA extraction or histological analysis.

RESULTS

PLAGL1 Binds a Different Consensus Sequence than PLAG1 and PLAGL2. To compare the DNA-binding specificities of the PLAG proteins, we performed EMSA analysis on double-strand probes containing either the PLAG1 consensus binding site (WT2 probe), the PLAGL1 consensus binding site (zac probe; Ref. 8), or on five mutated probes (see Fig. 1). The proteins used for this study were full-length PLAG proteins translated *in vitro* in reticulocyte lysates. As shown in a previous study (4), we found that PLAG1 binds strongly to the PLAG1 consensus-binding motif (Fig. 1A, Lane 1). Mutations in the G-cluster reduce drastically the binding (Fig. 1A, Lane 2), whereas destruction of the Core abolishes it (Fig. 1A, Lane 3) as do mutations in both (Fig. 1A, Lane 4). The distance between the G-cluster and the Core was also shown to be important, as PLAG1 only binds weakly to a probe containing the G-cluster separated by 2 bp instead of 7 bp from the Core (Fig. 1A, Lane 5). In contrast, the binding of PLAG1 to the zac probe (Fig. 1A, Lane 6) is much less efficient than to the WT2 probe. A similar binding profile is observed with PLAGL2 (Fig. 1C, Lanes 1-7) suggesting that PLAGL2 has binding capacities comparable with PLAG1. In contrast, PLAGL1 show different binding specificities, as it binds more efficiently to the zac probe than to the WT2 probe (compare Fig. 1B, Lane 6 to Lane 1). Moreover, mutations in the cluster of WT2 only slightly affect PLAGL1 binding (Fig. 1B, Lane 2), suggesting that a G-cluster is not critical for the binding of PLAGL1. This hypothesis is corroborated by the fact that the zac probe does not contain any G-cluster. Mutations in the core motif of the PLAG1 consensus, on the other hand, completely prevent the binding of PLAGL1 (Fig. 1B, Lane 3) as well as mutations in the core of the zac probe. Comparable results were also obtained using chimeric proteins containing the complete zinc finger domain of PLAG proteins fused in-frame to glutathione *S*-transferase (data not shown). All of these results indicate that both motifs, the core and the G-cluster, are critical for PLAG1 and PLAGL2 binding, whereas only the core motif is recognized by PLAGL1.

Fingers 3 of PLAG1 and PLAGL2 but not of PLAGL1 Are Critical for the DNA-binding Capacities. We have shown recently that finger 3 of PLAG1 interacts with the G-cluster, whereas the core is recognized by fingers 6 and 7 (4). As the G-cluster is critical for the binding of PLAG1 and PLAGL2 but not for PLAGL1, we were interested in determining whether finger 3 could play different roles in these three proteins. To answer this question, we produced mutant PLAG proteins where finger 3 was destroyed by replacing the first histidine of the C₂H₂ motif with an alanine. This mutation hinders the coordination of zinc and has been shown to prevent the formation of a functional zinc finger (16). The destruction of finger 3 in PLAG1 and in PLAGL2 drastically reduces the affinity of these proteins for the WT2 probe (compare Lanes 8 with Lanes 1 in Fig. 1, A and C). The specificity is also completely modified because the F3mut protein binds equally well to WT2, mCLU2, and WT2ml (Lanes 9, 10, and 12 in Fig. 1, A and C). Moreover, the F3mut binds preferentially to the zac probe compared with the WT2 probe (compare Lanes 13 and 8 in Fig. 1, A and C). These results indicate that, as for PLAG1, finger 3 of PLAGL2 is required for interaction with the G-cluster. On the contrary, destruction of finger 3 of PLAGL1 does not affect the binding specificity of this protein and only slightly decreases its affinity (compare Lanes 8-14 in Fig. 1B with Lanes 1-7). This indicates that in contrast to PLAG1 and PLAGL2, finger 3 of PLAGL1 is not directly involved in DNA recognition.

Fig. 1. *PLAGL1* binds a different consensus sequence to *PLAG1* and *PLAGL2*. EMSAs were performed with recombinant *PLAG* proteins produced *in vitro* in reticulocyte lysates. *PLAG* proteins were incubated with the probes WT2 (Lanes 1 and 8), mCLU2 (Lanes 2 and 9), mCO₂ (Lanes 3 and 10), mCLUmCO₂ (Lanes 4 and 11), WT2m1 (Lanes 5 and 12), Zac (Lanes 6 and 13), and Zac mut (Lanes 7 and 14) as described in "Materials and Methods." Equal efficiencies of protein expression were obtained for the different constructs as demonstrated by SDS-PAGE of proteins labeled with [³⁵S]methionine (data not shown). The percentage of binding of the *PLAG* proteins to the different probes were compared with the binding of the wild-type *PLAG* to the probe WT2 and are the means of at least two experiments. *, a band attributable to binding to the WT2 probe of a protein present in the reticulocyte lysate.

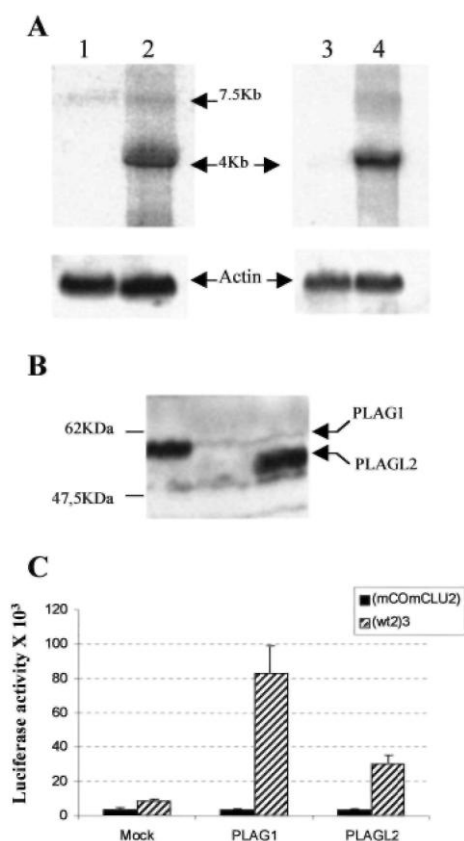


NIH3T3 Cells Infected with Retrovirus-containing Human *PLAG1* and *PLAGL2* cDNAs Express High Levels of Functional Proteins. To generate NIH3T3 cell lines overexpressing *PLAG1* and *PLAGL2*, we infected the cells with the pMSCV retroviral vector encoding FLAG-tagged human *PLAG1* or *PLAGL2*. Empty pMSCV vector was used as a negative control. Positive transformants were obtained by puromycin selection and checked for gene expression by Northern blot and Western blot analyses. As shown on Fig. 2A, the exogenous

PLAG1 and *PLAGL2* messages expressed from the viral 5' long terminal repeat could be detected as a 4-kb transcript in infected cells (Fig. 2A, Lanes 2 and 4, respectively) but not in mock infected control cells (Fig. 2A, Lanes 1 and 3). These are clearly overexpressed compared with the endogenous transcripts. The endogenous *PLAG1* transcript is visible as a 7.5-kb band (Fig. 2A, Lanes 1 and 2), whereas the endogenous *PLAGL2* transcript, which is also expected to be 7.5 kb, was undetectable (Fig. 2A, Lanes 3 and 4), suggesting extremely low expression, if any, of endogenous *PLAGL2*. Western blot analysis was performed to detect the presence of *PLAG1* and *PLAGL2* recombinant proteins in infected NIH3T3 cells (Fig. 2B). A M_r 56,000 and a M_r 50,000 protein corresponding to *PLAG1* (Fig. 2B, Lane 1) and *PLAGL2* (Fig. 2B, Lane 3), respectively, were present in infected cells but absent in mock-infected control cells (Fig. 2B, Lane 2). These proteins were shown to be functional, because *PLAG1*- and *PLAGL2*-overexpressing cells can stimulate the luciferase activity of a reporter construct containing three copies of the consensus binding site (WT2)₃-TK luc (27- and 10-fold, respectively; Fig. 2C). This stimulation is completely abolished when the core and cluster are mutated (mCOMCLU). In contrary, mock-infected cells only slightly induced the (WT2)₃-TK luc reporter construct (~2.5-fold). This induction is probably because of endogenous *PLAG1* present in the NIH3T3 cells.

All of these data indicate that infected NIH3T3 cells produce high level of functional *PLAG1* and *PLAGL2* proteins. Moreover, it is the first demonstration that *PLAGL2* is also a genuine transcription factor.

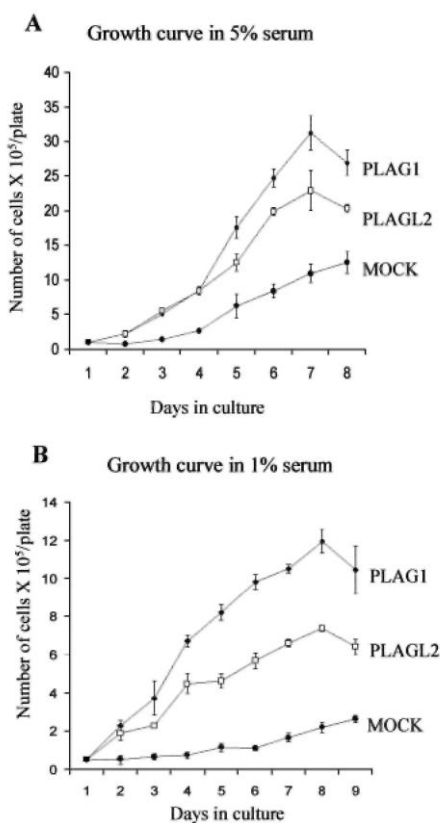
Fig. 2. NIH3T3 cells infected with recombinant retrovirus containing human *PLAG1* or *PLAGL2* express high levels of functional protein. A, total RNA from NIH3T3 cells infected with control virus (Lanes 1 and 3), human Flag-*PLAG1* retrovirus (Lane 2), and human Flag-*PLAGL2* retrovirus (Lane 4) were hybridized with a ³²P-labeled human *PLAG1* cDNA (Lanes 1 and 2) or with a ³²P-labeled human *PLAGL2* cDNA (Lanes 3 and 4). Expression of β -actin monitored the integrity and yield of RNA. B, Western blot analysis of whole cell lysates from NIH3T3 cells infected with Flag-*PLAG1* retrovirus (Lane 1), control retrovirus (Lane 2), and Flag-*PLAGL2* retrovirus (Lane 3) using an α -FLAG mouse monoclonal antibody. C, *PLAG1* and *PLAGL2* can stimulate transcription through the binding to the consensus sequence WT2. Mock-, *PLAG1*-, and *PLAGL2*-expressing NIH3T3 cells were transfected with 400 ng of the (mCOMCLU2)₃ TK-luc reporter construct (■) and 400 ng of the (WT2)₃TK-luc reporter construct (▨), respectively. Rous Sarcoma Viral promoter- β -gal (200 ng) was cotransfected as internal control. The results correspond to the mean of the corrected luciferase value of at least two independent transfections performed in triplicate; bars, \pm SE.



Mitogenic Stimulation of NIH3T3 Cells Overexpressing

PLAG1 and PLAGL2. Transformed cells, unlike normal cells, are able to proliferate in culture medium containing low levels of serum, because they have become independent of growth factors. To prove that *PLAG1* and *PLAGL2* are transforming factors, we investigated the growth of NIH3T3 cells overexpressing *PLAG1* and *PLAGL2* in low serum culture conditions. Fig. 3A shows the growth curve of a population of cells grown in 5% FCS. The proliferation rate of cells overexpressing *PLAG1* and *PLAGL2* was significantly higher than mock-infected NIH3T3 cells (~3-fold for *PLAG1*- and 2.5 fold for *PLAGL2*-expressing cells). The effect was even more striking when cells were cultured in 1% FCS. *PLAG1*- and *PLAGL2*-expressing cells proliferate, whereas mock-infected NIH3T3 cells are unable to grow (Fig. 3B). The *PLAG1*-overexpressing cells consistently show higher growth rates than the *PLAGL2*-expressing cells. These data suggest that NIH3T3 cells over-expressing *PLAG1* and *PLAGL2* behave like transformed cells and lose dependence on growth factors present in FCS.

Fig. 3. The mitogenic stimulation of NIH3T3 cells overexpressing *PLAG1* and *PLAGL2*. Mock-, *PLAG1*-, and *PLAGL2*-expressing NIH3T3 cells were grown in DMEM supplemented with either 5% (A) or 1% (B) FCS and counted daily. After 7 days, *PLAG1*- and *PLAGL2*-expressing cells reached a maximum cell density. The data correspond to the mean of three independent experiments; bars, \pm SE.

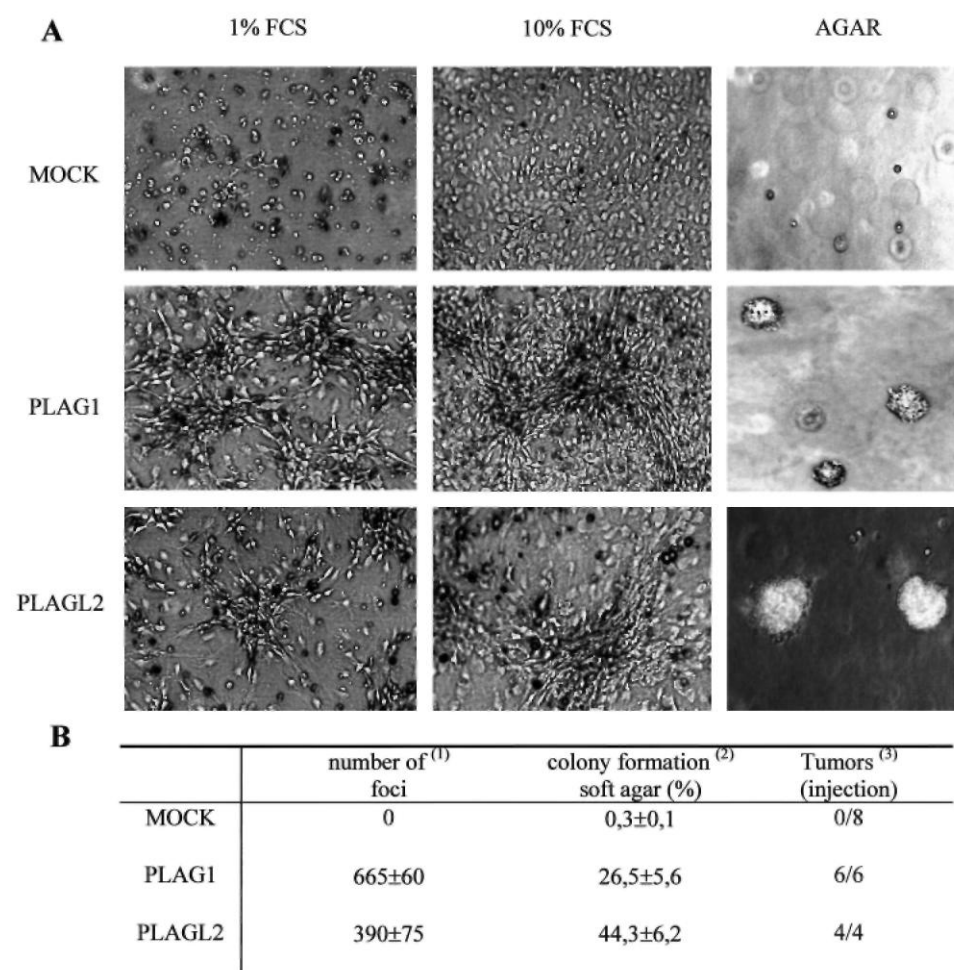


Overexpressed PLAG1 and PLAGL2 Proteins Are Able to Transform NIH3T3 Cells. To evaluate the transforming activity of *PLAG1* and *PLAGL2* when overexpressed, infected cells were grown as a monolayer to confluence in medium containing either 1% or 10% serum, and the formation of foci was analyzed (Fig. 4A). Contact inhibition of growth was lost leading the cells to pile up and form foci. Cells in the foci presented various morphologies, ranging from an elongated shape at the foci border to a rounded and refractile appearance in the center. *PLAG1*-expressing cells seemed to have a higher efficiency in forming foci than *PLAGL2*-expressing cells (Fig. 4A and B); foci appeared sooner and became much bigger. Foci were more rapidly observed in cells grown in medium containing 1% serum. In contrast, mock-infected NIH3T3 cells in both FCS concentrations exhibited contact inhibition and formed no foci. To test if *PLAG1*- and *PLAGL2*-mediated effects on growth and transformation are dependent on their DNA binding activity, we made retroviral constructs of *PLAG1* and *PLAGL2* containing a mutation in finger 7 to destroy their binding to DNA (4). NIH3T3 cells were

infected with these retro-viruses, and focus-forming assay was performed. Transformation of the NIH3T3 cells was almost completely abolished supporting the hypothesis that the transformation is caused by binding and subsequently activation of the target genes of *PLAG1* and *PLAGL2* (data not shown).

The cell lines overexpressing *PLAG1* and *PLAGL2* were also tested for anchorage-independent growth, another tumorigenic feature. For this, cells were seeded in a soft agar suspension and colonies counted 3 weeks after growth. Colonies first appeared microscopically 10 days after seeding. Colonies of *PLAG1*-expressing cells remained small compared with colonies formed in *PLAGL2*-overexpressing cells where the cells were able to form colonies visible by the naked eye within 4 weeks of incubation (Fig. 4A). *PLAGL2*-expressing cells showed a colony-forming efficiency of 44%, whereas for *PLAG1*-expressing cells, 26% of seeded cells give rise to colonies (Fig. 4B). As expected, control cells failed to form such colonies. These results are summarized in Fig. 4B.

Fig. 4. Overexpressed *PLAG1* and *PLAGL2* proteins are able to transform NIH3T3 cells. A, the mock-, *PLAG1*-, and *PLAGL2*-expressing NIH3T3 cells were used for focus-forming assay in medium containing 1% FCS or 10% FCS and for soft agar assay as described in "Materials and Methods." The photographs ($\times 100$ magnification) were taken on day 17 (focus assay) and day 25 (agar). B, table of the transforming properties of the NIH3T3 transfectants: the number of foci per 300 000 puromycin-resistant cells. Average of three dishes from two independent infection experiments from cells grown in 1% FCS (1). Colonies have been counted 24 days after seeding and results are expressed as the ratio [(number of colonies formed/ number of plated cells) $\times 100$] (2). The number of tumors per site of inoculation (3).



PLAG1- and PLAGL2-expressing NIH3T3 Cells Are Tumorigenic in Nude Mice. To determine whether the *PLAG1*- and *PLAGL2*-expressing NIH3T3 cells are tumorigenic in nude mice, cells were injected s.c. into athymic NMRI-*nu/nu* mice and examined every week for tumor development. *PLAG1*-overexpressing cells induced rapidly growing tumors at the site of inoculation within 3 weeks, whereas tumor formation originating from cells overexpressing *PLAGL2* was apparent a few days later. The mock-infected cells did not form any tumors during this time period (Fig. 4B). The mice were sacrificed after 5 weeks, and histological analysis identified tumors induced by the *PLAG1*-expressing cell line as fibrosarcomas (data not shown). Metastatic spread to other organs was not detected macroscopically during the time period of observation, but formation of microscopic metastasis cannot be ruled out. To verify whether *PLAG1* and *PLAGL2* were still expressed in the tumor, Northern blot analysis was performed. High levels of retroviral *PLAG1* and *PLAGL2* transcripts could be detected indicating that the tumors produced in the nude mice originated from the injected cells (data not shown).

IGF-II Is Up-Regulated in Cells Overexpressing PLAG1 and PLAGL2. As shown in this report, *PLAG1* and *PLAGL2* have common transcriptional properties, because they activate transcription via binding to the same DNA consensus sequence. These observations indicate that *PLAG1* and *PLAGL2* could be transcription factors that regulate common genes. Because *IGF-II* has been identified as a putative target gene of *PLAG1*, we analyzed *IgfII* expression in *PLAG1*- and *PLAGL2*-overexpressing NIH3T3 cells. As shown in Fig. 5, a significant up-regulation of the major *IgfII* transcript was observed in cells overexpressing *PLAG1* and *PLAGL2* (Fig. 5, lanes b and c). In addition, two minor transcripts of 2.0 and 1.2 kb, not present in the control cells, were also detected in cells overexpressing *PLAG1* and *PLAGL2*. Moreover, *PLAGL2* induces *IgfII* expression in the same range as *PLAG1*. To exclude the possibility that *IgfII* up-regulation in transformed NIH3T3 cells could be a secondary effect occurring in the process of the transformation, we determined whether *IGF-II* constitutes a transcriptional target for *PLAG1* and *PLAGL2*. For this purpose, we generated *PLAG*-inducible cell lines where *IGF-II* expression could be analyzed shortly after induction of *PLAG1* and *PLAGL2* expression. We isolated independent clones, deriving from the human epithelial kidney 293 cell line, containing a zinc-inducible expression vector (11) encoding either *PLAG1* (clones P1-8 and P1-32), *PLAGL2* (clones PL2-2 and PL2-24), or the *lacZ* gene (clones B-1 and B-4). When clones were grown in the absence of zinc ions, no exogenous *PLAG1* or *PLAGL2* could be detected, whereas only low level of β -gal were detected. On induction with 100 μ M of $ZnCl_2$, *PLAG1* and *PLAGL2* transcripts are efficiently synthesized. This expression results in a drastic up-regulation of *IGF-II* expression (Fig. 6). This stimulation is specific, because it is not observed either with the β -gal-expressing clones used as control or with the parental cell line. Furthermore, *IGF-II* up-regulation by *PLAGL2* goes not via the induction of endogenous *PLAG1* and *vice versa*, because no stimulation of endogenous *PLAG1* and *PLAGL2* transcript could be detected after zinc induction (data not shown). Moreover, the detected 6-kb *IGF-II* transcript corresponds to the one deriving from the P3 promoter, which is known to contain *PLAG1*-binding sites (4), as hybridization with a probe specific for the P3 transcript (exon 5 probe) detects the same band (data not shown). All of these results demonstrate a strong correlation between *PLAG1*, *PLAGL2*, and *IGF-II* expression, suggesting that *IGF-II* is a target gene not only for *PLAG1* but also for *PLAGL2*.

Fig. 5. *IgfII* is up-regulated in NIH3T3 cells overexpressing *PLAG1* and *PLAGL2*. Northern blot analysis of total RNA extracted from NIH3T3 cells infected with empty virus (a), human Flag-*PLAG1* (b), and human Flag-*PLAGL2* (c) grown in 10% FCS. The membrane was hybridized with a ³²P-labeled mouse *IgfII* probe specific for exon 6, a ³²P-labeled *PLAG1* probe, or a ³²P-labeled *PLAGL2* probe. Expression of β -actin transcript monitored the integrity and yield of RNA.

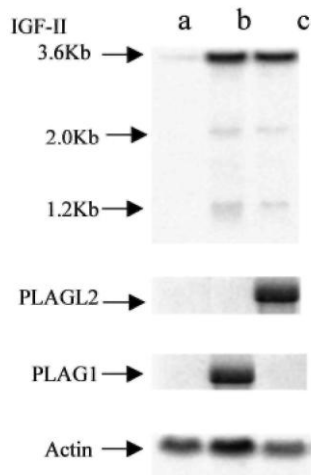
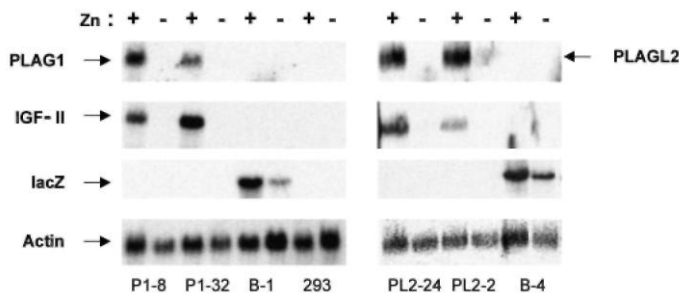


Fig. 6. *IGF-II* is a direct target of *PLAG1* and *PLAGL2*. Northern blot analysis of total RNA isolated from clones, deriving from the human epithelial kidney 293 cell line, containing a zinc-inducible expression vector (11) either for *PLAG1* (clones P1-8 and P1-32), *PLAGL2* (clones PL2-2 and PL2-24), or the *lacZ* gene (clones B-1, B21, and B-4) grown without (-) or with (+) 100 μ M of $ZnCl_2$. Blots were hybridized sequentially with ³²P-labeled human *PLAG1* cDNA, ³²P-labeled human *PLAGL2* cDNA, ³²P-labeled *lacZ*, ³²P-labeled human *IGF-II* probe, and ³²P-labeled human actin probe.



DISCUSSION

Pleomorphic adenomas of the salivary glands are characterized by recurrent translocations that lead to promoter substitution between *PLAG1*, a gene mainly expressed in fetal tissue, and more broadly expressed genes. The replacement of the *PLAG1* promoter, inactive in adult salivary glands, by a strong promoter derived from the translocation partner leads to ectopic expression of *PLAG1* in tumoral cells (1). The question remains whether ectopic expression of *PLAG1* leads to the development of neoplasias, in this way acting as an oncogene. To approach this question, we determined the *in vitro* transforming capacity of *PLAG1* in NIH3T3 cells. The transformation of NIH3T3 cells is a sensitive bioassay for the detection of transforming genes (17). Since we also show here that *PLAGL2* has indistinguishable DNA-binding capacities compared with *PLAG1*, we were interested to see if *PLAGL2* has the same transforming effect *in vitro*. We found that cell lines producing high levels of *PLAG1* or *PLAGL2* are able to proliferate in medium containing only 1% serum suggesting that these genes partially abrogate the serum requirement for the growth of NIH3T3 cells. Moreover, these cells expressed the typical markers of neoplastic transformation; foci appeared within 2-3 weeks with a similar morphology to that described previously in transfection studies involving integrated c-ets1 DNA in NIH3T3 cells (18). In addition, cells overexpressing *PLAG1* and *PLAGL2* show anchorage-independent growth and are able to induce tumors in nude mice. These observations allow us to define the *PLAG1* and *PLAGL2* family members as proto-oncogenes with mitogenic and transforming potential when overexpressed in NIH3T3 cells. On the contrary, the

PLAGL1 family member has been shown to inhibit tumor cell proliferation through induction of both apoptosis and cell cycle arrest, in this way acting as a tumor suppressor gene (8). These data together with our own indicate that the three members of the *PLAG* family are involved in cellular transformation in distinct ways.

The *in vitro* transformation data are consistent with the role of *PLAG1* and *PLAGL1* described in tumorigenesis. Indeed, *PLAGL1* prevents the proliferation of tumor cells *in vitro* (8, 19), which correlates with the complete or partial loss of *PLAGL1* expression observed in breast tumor cell lines and primary breast tumors harboring loss of chromosomal material in the 6q24-25 region. This suggests that loss of expression of *PLAGL1* in premalignant epithelial cells can contribute to the initiation or progression of breast tumors (9). For *PLAGL1*, the *in vitro* data indicate that *PLAG1* is able to induce cellular transformation when overexpressed. This correlates with *in vivo* data, because *PLAG1* ectopic expression was observed not only in pleomorphic adenomas of the salivary gland but also in other kinds of tumors. Indeed, *PLAG1* promoter swapping has been discovered recently to also be a critical event in lipoblastomas with 8q12 rearrangements (20). Ectopic expression has also been found in other tumors such as uterine leiomyoma, leiomyosarcomas, and smooth muscle tumors, and in pleomorphic adenomas with 12q15 translocations and normal karyotype (3). This emphasizes the importance of *PLAG1* overexpression in tumorigenesis. Regarding *PLAGL2*, thus far we have no evidence for aberrant expression in any type of tumor. However, chromosome 20q11-12 aberrations, in the region where *PLAGL2* is located, are a recurrent abnormality in malignant myeloid disorders. By screening the tumor databank of the Center for Human Genetics in Leuven, 20q11-12 translocations were found in patients who developed myeloid diseases. Fluorescence *in situ* hybridization analysis revealed that three patients present translocations in the *PLAGL2* region. Additional investigations are still required to determine whether *PLAGL2* overexpression could play a role in the development of this disease.

The mechanisms by which *PLAG1* and perhaps *PLAGL2* proteins induce tumorigenesis are not yet known. Because *PLAG1* and *PLAGL2* are genuine transcription factors, deregulation of *PLAG* expression possibly leads to deregulation of particular target genes involved in mitogenic stimulation, tissue remodeling, and vascularization associated with neoplasias. In this report we show that *IgfII* is not only up-regulated in NIH3T3 cells expressing *PLAG1* and *PLAGL2*, but *IGF-II* expression is also immediately activated on *PLAG1* and *PLAGL2* expression by using *PLAG1* and *PLAGL2* zinc-inducible human 293 kidney cell lines. These results suggest that *IGF-II* is a target gene of *PLAG1* and *PLAGL2*. *IGF-II* is a peptide fetal growth factor that plays an important role during embryonic development and carcinogenesis (21). Interestingly, the pattern of expression of *PLAG1* and *IGF-II* is similar because expression is high during fetal life and decreases drastically after birth (22, 23).² These results link abnormal *PLAG1* and *PLAGL2* expression with the activation of the *IGF-II* mitogenic signaling, which is mainly mediated via the IGF-I-R. Activation of the IGF-I-R can increase mitogenesis, which is mediated primarily by activating the Ras/Raf/ mitogen-activated protein kinase pathway (24). This provides an explanation for the ability of *PLAG1* and *PLAGL2* to stimulate neoplastic transformation. This hypothesis is supported by transformation studies performed on R⁻ cells. R⁻ cells are 3T3 cells derived from mouse embryos with a targeted disruption of the IGF-I-R genes (25, 26). Because the transforming effect of IGF-II is believed to be mainly mediated via this receptor, we were wondering if *PLAG1* and *PLAGL2* still could transform these R⁻ cells. When focus-forming assay was performed on R⁻ cells overexpressing *PLAG1* or *PLAGL2*, cells could not form foci anymore (data not shown). We can now propose a model that ectopic expression of *PLAG1* and *PLAGL2* leads to the reactivation of *IGF-II* transcription, which results in a restarted developmental program with concomitant loss of differentiation, the typical hallmark of any tumor. This model is supported by immunohistochemistry on pleomorphic adenomas of the salivary gland. It revealed that the most differentiated cells of the inner tubuloductal epithelium only sporadically express *PLAG1*, whereas less differentiated cells of the outer tubuloductal epithelium in the tumor were strongly *PLAG1* positive (27). Moreover, undifferentiated cells in the tumor exhibited up-regulation of the antiapoptotic Bcl2 protein, a downstream element in the cascade of the antiapoptotic activity mediated via the IGF-I-R. Indeed, the transforming activity of the IGF-I-R depends on its potent antiapoptotic activity in addition to its mitogenic effect (28, 29). Additional investigations will be performed to analyze which level of the IGF system is influenced in *PLAG1*-mediated tumorigenesis.

As shown here, all of the three members of the *PLAG* family seem to be involved in tumorigenesis but in distinct ways. This difference in function is reflected in the DNA-binding capacity, because we found that the *PLAG* proteins display different binding characteristics. Indeed, *PLAG1* and *PLAGL2* bind to a bipartite motif containing a Core and the G-cluster, whereas *PLAGL1* binds only to an extended Core motif (Fig. 7B). This difference can be explained by the fact that the finger 3 of *PLAGL1* is not directly involved in DNA recognition, whereas in *PLAG1* and *PLAGL2*, it interacts with the G-cluster. This difference in binding specificity is quite surprising, as the zinc finger domain of the three *PLAG* proteins is quite highly conserved (74% identity; Fig.

² Hensen *et al.*, unpublished observations

7A). The highest homology is found in fingers 6 and 7, responsible for binding to the Core motif. This can explain why these three proteins recognize a similar Core sequence (Fig. 7B). In contrast, fingers 2 to 5 shows much less conservation except in the key residues (highlighted in Fig. 7A). These residues typically make key base contacts that are responsible for defining sequence specificity (reviewed in Ref. 30). Finger 3, which is critical for the binding to the G-cluster, is surprisingly well conserved in PLAGL1, notably in the key residues (see Fig. 7A). This indicates that these key residues, although essential for binding, are not sufficient to determine specificity and that other amino acids also play a role.

It is interesting to note that PLAG1 undergoes extensive alternative splicing, notably of exon 4, which contains the first ATG (31). This will lead to different isoforms starting either at methionine 83 or methionine 100. This is assumed to have considerable consequences, because the isoform starting at position 100 does not contain finger 3 and, thus, does not recognize the G-cluster, giving rise to a splice form with different DNA binding specificity. This is reminiscent of the situation of the Wilms tumor 1 gene (32) and the PR-domain family genes (33) where the different isoforms have different DNA specificities and even opposing effects on tumorigenicity.

On the basis of our DNA-binding studies, we can also hypothesize that the difference in DNA-binding specificity described here could be one of the reasons *PLAGL1* behaves as a tumor suppressor gene in contrast to the other two family members. *PLAGL1* probably regulates a different set of target genes, which results in a different response. Regarding PLAG1 and PLAGL2, their similar binding capacities suggest that they regulate the expression of the same target genes, and *IGF-II* is the first example of such a common target gene. This discovery of *IGF-II* as a target in pleomorphic adenomas is an important step in the treatment of this disease, because we can envision that drugs designed to decrease the *IGF-II* levels in other types of tumors could be also used for the treatment of pleomorphic adenomas.

Fig. 7. Comparison of the zinc finger motifs in the three PLAG proteins. A, alignment of the seven zinc fingers motifs in PLAG1, PLAGL1, and PLAGL2. Only the amino acids different in PLAGL1 and PLAGL2 are indicated. The key residues (highlighted) are defined on the basis that each finger module folds to form a compact $\beta\beta\alpha$ structure with the α -helix fitting in the major groove. (reviewed in Ref. 30). Residues -1, +2, +3 and +6 (numbering with respect to the start of the α -helix) typically make key base contacts that are responsible for defining sequence specificity. B, comparison of the DNA-binding consensus sequence of PLAG1 and PLAGL1. The consensus reported here for PLAG1 is not the minimal consensus GRGGC(N)7RGGK as described previously (4) but has been extended on both sides of the Core by the more frequent bases found in the CASTing experiments.

A)		-1 23 6
PLAG1 finger 1	FPC..QLCDKAFNSV E KLKVHSYS.HTGERP	
PLAGL1	G T LTL FTI N SR	
PLAGL2	.QC EISGTP SNG R P LP.QPEQ	
PLAG1 Finger 2	YKCIQQDCTKAFV S K K LQ R HMAT.HSPEKT	
PLAGL1	V P G R M Q S	
PLAGL2	S P LH G A Y AQ P	
PLAG1 Finger 3	HKC..NYCEKMP F R K DELK N HLHT.HDPNKET	
PLAGL1	Q AH T N FQ MA	
PLAGL2	Q M D R Q A	
PLAG1 Finger 4	FKCEE..CGKNY N T K L G F K RHLAL.HAATSGD	
PLAGL1	G K M Y S	
PLAGL2	LH S YR M S	
PLAG1 Finger 5	LTC..KVCLQTF E S T G V L L EHLKS.HAG.KSSGGVKEKK	
PLAGL1	G ALELG E D A EE PPS T	
PLAGL2	S Q A A SR.RVA A	
PLAG1 Finger 6	HQCEH..CDRRFY T R D V R RHMVV.HTGRKD	
PLAGL1	D E C L C	
PLAGL2	P D L	
PLAG1 Finger 7	FLC..OYCAOR F R K DEL T RHMKKSHNQELL	
PLAGL1	F T T S	
PLAGL2	V S	
C2H2 Consensus	FxCxxxxCxxxFxxxxxLxx H xxxx H xxxxx	
B)	Zac1	GGGGGGCCCC
	PLAG1	GGGGCCNNNNNNRGGK

ACKNOWLEDGMENTS

We thank Prof. Dr. B. Van Damme for the histological analysis of the tumors from the nude mice, Jan Cools from the CME KULeuven for providing the pMSCVpuro and pIK6.1 Ecopac vector and technical advice, N. Agten and M. Willems for the technical assistance, P. E. Holthuisen for her kind gift of the *IGF-II* exon5 probe, Dr. J. Rossant for her kind gift of the SDKlacZpA vector, Bert Vogelstein for the kind gift of the pSAR-MT- β gal vector, and Dr. Renato Baserga from the Kimmel Cancer Center at the Thomas Jefferson University in Philadelphia, PA, for providing the R⁻ cells. Additionally, we thank Neil Taylor for critical review of the manuscript.

REFERENCES

1. Kas, K., Voz, M. L., Roijer, E., Astrom, A. K., Meyen, E., Stenman, G., and Van de Ven, W. J. Promoter swapping between the genes for a novel zinc finger protein and β -catenin in pleiomorphic adenomas with t(3;8)(p21;q12) translocations. *Nat. Genet.*, 15: 170-174, 1997.
2. Voz, M. L., Astrom, A. K., Kas, K., Mark, J., Stenman, G., and Van de Ven, W. J. The recurrent translocation t(5;8)(p13;q12) in pleiomorphic adenomas results in up-regulation of PLAG1 gene expression under control of the LIFR promoter. *Oncogene*, 16: 1409-1416, 1998.
3. Astrom, A. K., Voz, M. L., Kas, K., Roijer, E., Wedell, B., Mandahl, N., Van de Ven, W., Mark, J., and Stenman, G. Conserved mechanism of PLAG1 activation in salivary gland tumors with and without chromosome 8q12 abnormalities: identification of SII as a new fusion partner gene. *Cancer Res.*, 59: 918-923, 1999.
4. Voz, M. L., Agten, N. S., Van de Ven, W. J., and Kas, K. PLAG1, the main translocation target in pleiomorphic adenoma of the salivary glands, is a positive regulator of IGF-II, *Cancer Res.* 60: 106-113, 2000.
5. Kas, K., Voz, M. L., Hensen, K., Meyen, E., and Van de Ven, W. J. M. Transcriptional activation capacity of the novel PLAG family of zinc finger proteins. *J. Biol. Chem.*, 273: 23026-23032, 1998.
6. Abdollahi, A., Roberts, D., Godwin, A. K., Schultz, D. C., Sonoda, G., Testa, J. R., and Hamilton, T. C. Identification of a zinc-finger gene at 6q25: a chromosomal region implicated in development of many solid tumors. *Oncogene*, 14: 1973-1979, 1997.
7. Spengler, D., Villalba, M., Hoffmann, A., Pantaloni, C., Houssami, S., Bockaert, J., and Journot, L. Regulation of apoptosis and cell cycle arrest by Zacl, a novel zinc finger protein expressed in the pituitary gland and the brain. *EMBO J.*, 16: 2814-2825, 1997.
8. Varrault, A., Ciani, E., Apiou, F., Bilanges, B., Hoffmann, A., Pantaloni, C., Bockaert, J., Spengler, D., and Journot, L. hZAC encodes a zinc finger protein with antiproliferative properties and maps to a chromosomal region frequently lost in cancer. *Proc. Natl. Acad. Sci. USA*, 95: 8835-8840, 1998.
9. Bilanges, B., Varrault, A., Basyuk, E., Rodriguez, C., Mazumdar, A., Pantaloni, C., Bockaert, J., Theillet, C., Spengler, D., and Journot, L. Loss of expression of the candidate tumor suppressor gene ZAC in breast cancer cell lines and primary tumors. *Oncogene*, 18: 3979-3988, 1999.
10. Hawley, R. G., Lieu, F. H., Fong, A. Z., and Hawley, T. S. Versatile retroviral vectors for potential use in gene therapy. *Gene Ther.*, 1: 136-138, 1994.
11. Morin, P. J., Vogelstein, B., and Kinzler, K. W. Apoptosis and APC in colorectal tumorigenesis. *Proc. Natl. Acad. Sci. USA*, 93: 7950-7954, 1996.
12. Nordeen, S. K. Luciferase reporter gene vectors for analysis of promoters and enhancers. *Biotechniques*, 6: 454-458, 1988.
13. Chomczynski, P., and Sacchi, N. Single-step method of RNA isolation by acid guanidinium thiocyanate-phenol-chloroform extraction. *Anal. Biochem.*, 162: 156-159, 1987.
14. Dull, T. J., Gray, A., Hayflick, J. S., and Ullrich, A. Insulin-like growth factor II precursor gene organization in relation to insulin gene family. *Nature (Lond.)*, 310: 777-781, 1984.
15. Sanchez, M. P., Silos-Santiago, I., Frisen, J., He, B., Lira, S. A., and Barbacid, M. Renal agenesis and the absence of enteric neurons in mice lacking GDNF. *Nature (Lond.)*, 382: 70-73, 1996.
16. Ikeda, K., and Kawakami, K. DNA binding through distinct domains of zinc-finger-homeodomain protein AREB6 has different effects on gene transcription. *Eur. J. Biochem.*, 233: 73-82, 1995.
17. Jainchill, J. L., Aaronson, S. A., and Todaro, G. J. Murine sarcoma and leukemia viruses: assay using clonal lines of contact-inhibited mouse cells. *J. Virol.*, 4: 549-553, 1969.

18. Seth, A., and Papas, T. S. The c-ets-1 proto-oncogene has oncogenic activity and is positively autoregulated. *Oncogene*, 5: 1761-1767, 1990.
19. Abdollahi, A., Bao, R., and Hamilton, T. C. LOT1 is a growth suppressor gene down-regulated by the epidermal growth factor receptor ligands and encodes a nuclear zinc-finger protein. *Oncogene*, 18: 6477-6487, 1999.
20. Hibbard, M. K., Kozakewich, H. P., Dal Cin, P., Scot, R., Tan, X., Xiao, S., and Fletcher, J. A. PLAG1 fusion oncogenes in lipoblastoma. *Cancer Res.*, 60: 4869-4872, 2000.
21. Toretsky, J. A., and Helman, L. J. Involvement of IGF-II in human cancer. *J. Endocrinol.*, 149: 367-372, 1996.
22. Roberts, C. T., Jr., Brown, A. L., Graham, D. E., Seelig, S., Berry, S., Gabbay, K. H., and Rechler, M. M. Growth hormone regulates the abundance of insulin-like growth factor I RNA in adult rat liver. *J. Biol. Chem.*, 261: 10025-10028, 1986.
23. Brown, A. L., Graham, D. E., Nissley, S. P., Hill, D. J., Strain, A. J., and Rechler, M. M. Developmental regulation of insulin-like growth factor II mRNA in different rat tissues. *J. Biol. Chem.*, 261: 13144-50, 1986.
24. LeRoith, D., Werner, H., Neuenschwander, S., Kalebic, T., and Helman, L. J. The role of the insulin-like growth factor-I receptor in cancer. *Ann. N. Y. Acad. Sci.*, 766: 402-408, 1995.
25. Sell, C., Dumenil, G., Deveaud, C., Miura, M., Coppola, D., DeAngelis, T., Rubin, R., Efstratiadis, A., and Baserga, R. Effect of a null mutation of the insulin-like growth factor I receptor gene on growth and transformation of mouse embryo fibroblasts. *Mol. Cell. Biol.*, 14: 3604-3612, 1994.
26. Sell, C., Rubini, M., Rubin, R., Liu, J. P., Efstratiadis, A., and Baserga, R. Simian virus 40 large tumor antigen is unable to transform mouse embryonic fibroblasts lacking type 1 insulin-like growth factor receptor. *Proc. Natl. Acad. Sci. USA*, 90: 11217-11221, 1993.
27. Debiec-Rychter, M., Van Valckenborgh, I., Van Den Broeck, C., Hagemeyer, A., Van De Ven, W. J., Kas, K., Van Damme, B., and Voz, M. L. Histologic localization of plag1 (pleomorphic adenoma gene 1) in pleomorphic adenoma of the salivary gland: cytogenetic evidence of common origin of phenotypically diverse cells. *Lab. Investig.*, 81: 1289-1297, 2001.
28. Rodriguez-Tarduchy, G., Collins, M. K., Garcia, I., and Lopez-Rivas, A. Insulin-like growth factor-I inhibits apoptosis in IL-3-dependent hemopoietic cells. *J. Immunol.*, 149: 535-540, 1992.
29. Resnicoff, M., Burgaud, J. L., Rotman, H. L., Abraham, D., and Baserga, R. Correlation between apoptosis, tumorigenesis, and levels of insulin-like growth factor I receptors. *Cancer Res.*, 55: 3739-3741, 1995.
30. Choo, Y., and Klug, A. Physical basis of a protein-DNA recognition code. *Curr. Opin. Struct. Biol.*, 7: 117-125, 1997.
31. Queimado, L., Lopes, C., Du, F., Martins, C., Bowcock, A. M., Soares, J., and Lovett, M. Pleomorphic adenoma gene 1 is expressed in cultured benign and malignant salivary gland tumor cells. *Lab. Investig.*, 79: 583-589, 1999.
32. Menke, A. L., Riteco, N., van Ham, R. C., de Bruyne, C., Rauscher, F. J. d., van der Eb, A. J., and Jochemsen, A. G. Wilms' tumor 1 splice variants have opposite effects on the tumorigenicity of adenovirus-transformed baby-rat kidney cells. *Oncogene*, 12: 537-546, 1996.
33. Jiang, G. L., and Huang, S. The yin-yang of PR-domain family genes in tumorigenesis. *Histol. Histopathol.*, 15: 109-117, 2000.